Comparison between a silorane-based composite and methacrylate-based composites: Shrinkage characteristics, thermal properties, gel point and vitrification point

Bo-Tao GAO[1], Hong LIN[1], Gang ZHENG[1], Yong-Xiang XU[1] and Jin-Liang YANG[2]

[1]Department of Dental Materials, Peking University School and Hospital of Stomatology, 22 Zhongguanchun South Road, HaiDian District, Beijing 100081, China
[2]State Key Laboratory of Chemical Resource Engineering, College of Materials Science and Engineering, Beijing University of Chemical Technology, 15 Beisanhuan East Road, Chao Yang District, Beijing 100029, China
Corresponding author, Gang ZHENG; E-mail: zhengang101@126.com

A silorane-based composite was compared against methacrylate-based composites in terms of shrinkage characteristics, thermal properties, gel point, and vitrification point. Shrinkage strain was measured using a laser triangulation method. Shrinkage stress was measured using a stress analyzer. Heat flow during photopolymerization was measured using photo-DSC. Statistical analysis was performed using one-way ANOVA and Tukey's test (p=0.05). Silorane exhibited significantly lower shrinkage strain than the methacrylate-based composites. It also presented the lowest stress values during light exposure, but the highest maximum stress rate after light exposure. It showed the highest heat flow rate, and it took the longest time to reach gel and vitrification points. Silorane demonstrated improved performance over the methacrylate-based composites with delayed gel and vitrification points as well as reduced shrinkage strain and stress. However, a high quantity of heat was liberated during the curing process, causing silorane to show significantly higher stress rate (p<0.05) than the methacrylate-based composites after light exposure.

Keywords: Silorane-based composite, Methacrylate-based composite, Shrinkage

INTRODUCTION

During photopolymerization of a dental composite, it is transformed from a viscous fluid to an elastic gel at gel point. Vitrification, a phenomenon completely distinct from gelation, occurs after gel point when the elastic gel transforms to a glass. The latter transformation is accompanied by a significant development of shrinkage strain, increase in elastic modulus, and heat liberation. In clinical situations, the inevitable curing contraction of adhesive composites will result in shrinkage stresses if composite is efficiently bonded to the cavity walls of the restoration[1,2]. Such destructive shrinkage stresses of polymer-based adhesive restorative materials cause debonding at the restoration-tooth interface, resulting in a host of problems such as marginal leakage and secondary caries[3-5].

During curing, stress development generally undergoes different stages depending on the evolution of material mechanical stiffness. Before gel point, stress might be negligible because the material in pre-gel state can flow from the free surfaces to the bonded surface of restoration. As viscosity of a developing polymer is still low, shrinkage stress can thus be rapidly compensated. At gel point, a space-spanning, loading-bearing network forms. Stress should start to develop if material is constrained by adhesion to cavity walls of restoration. However, from gel point to vitrification point (rubbery regime), the modulus may remain low enough to lead only to a low stress. Moreover, any stress developed

relaxes quickly in the gel/rubbery state. When material enters the vitrified state, its elastic modulus becomes high and stress relaxation becomes slow. Stress development certainly becomes significant and faster if curing reaction proceeds in the vitrified state. Therefore, as material transits from gel point to vitrification point, high stress magnitude begins to emerge.

Several studies have attempted to characterize the gel and vitrification points of dental composites. Visvanathan et al.[6] proposed polymerization shrinkage force as an indirect measure of gel point, and that gel point was arbitrarily defined as the time needed to exceed a force threshold of 0.5 N. In the same vein, Fano et al.[7] proposed that the maximum shrinkage strain rate of resin composites occurred at gel point, citing the reason that auto-acceleration of polymerization rate was due to "gel effect"[8]. At gel point, shrinkage strain rate was at its highest because polymerization shrinkage was hindered by a build-up of three-dimensional networks of polymer chains, resulting in a dramatic physical change as well as dramatically improved mechanical and physical changes[7].

No generally accepted criteria and measurement protocols have been defined for monitoring and identifying vitrification points[9]. Nonetheless, it is established that polymerization of composite resins is an exothermic reaction, whereby heat emitted is a measure of the rate at which monomer molecules undergo chemical reaction to form polymer chains. Typically, rate of composite resin polymerization is at its highest before and at peak of heat release rate. This means that vitrification point can be defined as the time at which

peak heat flow rate is reached. Photo differential scanning calorimetry (Photo-DSC) has been employed to directly measure thermal changes which occur during the vitrification of composite resins. Heat flow reveals thermal characteristics, and the time taken to reach maximum heat flow rate is closely associated with normal vitrification times[10]. However, photo-DSC data lagged behind data obtained in stress and strain experiments. This is because instrumental inertia of the DSC cell prevented full heat evolution from being recorded.

Shrinkage stress development *per se* is a multi-factorial phenomenon, and stresses measured *in vitro* are further influenced by a host of multi-faceted factors: instrumental compliance of measurement system, cavity configuration factor (C-factor), as well as material's shrinkage strain, elastic modulus, gel and vitrification times[11]. A restoration's C-factor is the ratio of bonded surface area in a cavity to the unbonded surface area, and it has been shown to be closely related to shrinkage stress[11,12]. The higher the C-factor, the less unbonded or free surfaces there will be, leading to a situation where there is little chance for the composite to flow and accommodate contraction[12]. It is hard to change cavity configurations. To minimize shrinkage stress, alternative restorative techniques were explored and recommended.

For example, a suggested alternative curing technique is the "soft-start" technique. It employs an initial light activation at low irradiance followed by a second exposure at a higher irradiance[13]. The rationale is that a slower polymerization reaction would delay the gelation and vitrification of composite resin, thereby providing the latter with better ability to flow. This would result in reduced shrinkage stress and hence less damage at the adhesive interface[1]. Nonetheless, none of the proposed techniques to date could completely eliminate shrinkage stress. It seems that the surest way to avoid shrinkage stress is to use non-shrinking resins.

Low-shrinkage dental composites have been introduced to the market, amongst which is Filtek P90 (3M ESPE, St. Paul, MN, USA). According to the manufacturer, it is a silorane-based resin consisting of siloxane and oxirane functional moieties. When compared to methacrylate-based composites, the cycloaliphatic oxirane functional groups account for the lower shrinkage of siloranes. Oxiranes, which are cyclic ethers, polymerize *via* a cationic ring-opening mechanism; on the other hand, methacrylates polymerize *via* a free-radical mechanism[14].

Studies[15,16] on silorane-based composites have shown reduced volumetric shrinkage when compared to conventional methacrylate-based composites. However, there were studies[17,18] which reported that P90 did not show the lowest shrinkage stress among the tested composite materials. It was also reported that P90 registered a significantly higher temperature rise than the conventional methacrylate-based composites[19]. In light of these conflicting reports, it seemed that the silorane-based restorative material should be re-evaluated in terms of shrinkage behavior and thermal behavior against other currently available low-shrinkage composites.

The purpose of this *in vitro* study was to evaluate and compare a silorane-based restorative material with regular low-shrinkage composites in terms of shrinkage strain, shrinkage stress, stress rate, heat flow, gel and vitrification times. The tested hypothesis was that differences in the polymerization reaction mechanism of silorane-based composite cause it to display behaviors that are markedly different from methyacrylate-based composites.

MATERIALS AND METHODS

Composite materials
Table 1 lists the four composite materials tested in this study: a silorane-based restorative material [Filtek P90 (P9), 3M ESPE, St. Paul, MN, USA]; a low-shrinkage nanohybrid composite [Venus Diamond (VD), Heraeus Kulzer GmbH, Hanau, Germany]; a micro-filled composite [Durafill VS (DF), Heraeus Kulzer GmbH, Hanau, Germany]; and a universal microhybrid composite [Filtek Z250 (Z2), 3M ESPE, St. Paul, MN, USA]. All composite materials tested were of A3 shade.

Shrinkage strain measurement
1. Measurement setup
A laser triangulation method[20] was used to measure the

Table 1　Composite materials tested in this study

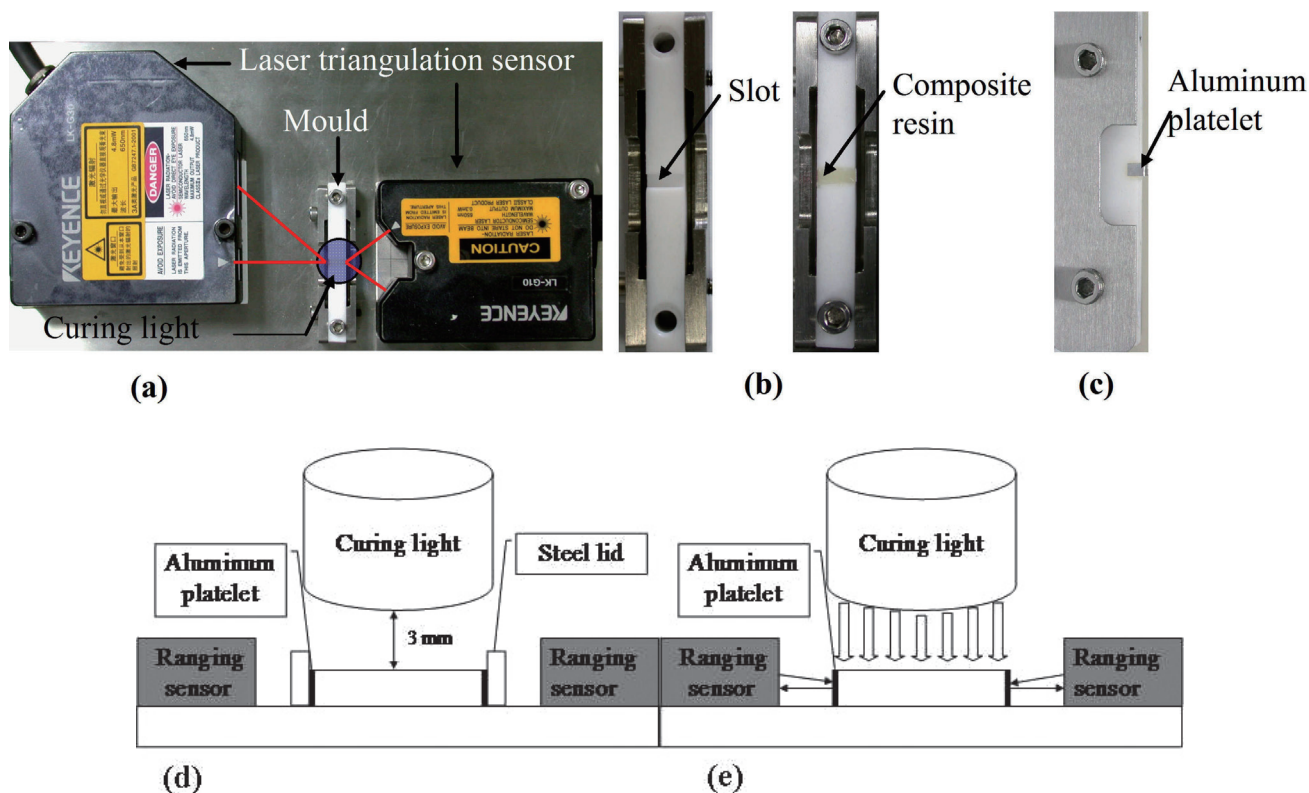| Composite	Batch	Filler (vol%)	Resin composition	Elastic modulus (GPa)
Filter P90 (P9) Silorane-based composite	N181887	53	Silorane	6.8[A]
Venus Diamond (VD) Nanohybrid composite	010028	64	TCD-DI-HEA, UDMA	4.5[A]
Durafill VS (DF) Micro-filled composite	21218	40	Bis-GMA, UDMA, TEGDMA	1.4[A]
Filter Z250 (Z2) Microhybrid composite	N227206	60	Bis-GMA, UDMA, Bis-EMA	5.6[A]

[A]: Reference 18)

Fig. 1   Shrinkage strain measurement setup (laser triangulation method): (a) Setup overview; (b) Composite specimen mounted in a slot in PTFE mold; (c) Thermally conductive aluminium platelets used for reflecting laser signals during LED light-curing; (d) Side view of setup before LED light-curing; (e) Side view of setup during LED light-curing.

axial shrinkage strain of composite specimens (Fig. 1). The measurement setup comprised two laser triangulation sensors (LK-G10 and LK-G30, Keyence Corp., Osaka, Japan) and two mounting pedestals, a composite specimen, a PTFE mold, and LED curing light (Bluephase, Ivoclar Vivadent, Schaan, Liechtenstein).

Composite specimen was mounted in a slot in PTFE mold. The two sensors were mounted on a pedestal each such that they were aligned with both ends of composite specimen (Fig. 1). In this way, polymerization shrinkage at both ends of specimen, within the same horizontal axis or in the same line, were measured at the same time. Total linear shrinkage strain of each composite specimen was the sum of shrinkage strain values at both ends.

Molded PTFE block allowed free shrinkage of composite specimen to take place because of absence of adhesion with the surfaces of both the bar and the mold. For specimen mounting, a rectangular slot of 2×2×6 mm (width×height×length) was cut out on the top surface of mold.

2. Measurement procedure

Both sides of the mold were covered with a steel lid each (Fig. 1d) to make the slot form an intact cavity. Next, two reflective aluminum platelets of 2 mm width × 2 mm height × 0.17 mm thickness were sandblasted and

treated with silane (Bisco Inc., Schaumburg, IL, USA) for 90 s to improve adhesion with the composite specimen. After surface conditioning, these two aluminum platelets were placed on both ends of the cavity respectively, leaning lightly against the steel lids (Figs. 1c and 1d).

Composite resin was inserted into the cavity, which was coated with a lubricant to allow the composite to shrink freely in the absence of any surface adhesion. As composite resin was compressed into the shape of a rectangular bar after insertion into the cavity, the aluminum platelets adhered to the composite specimen due to pressure and resin viscosity. Careful removal of the steel lids revealed a rectangular bar-like composite specimen (2 mm width×2 mm height×6 mm length) with its two free ends bonded to the aluminum platelets.

Laser beam emitted by each laser triangulation sensor was focused at the center of each aluminum platelet (Fig. 1e). Light-curing of composite specimen was performed from the top surface at 3 mm distance using the LED curing light (Bluephase) for 30 s at 650 mW/cm² (Fig. 1e). LK-Navigator (Keyence Corp., Osaka, Japan) was used to detect linear displacements, $i.e.$, changes in position or linear distance of the aluminum platelets and specimen for a duration of 600 s after start of irradiation (n=10 per composite material). Measurements were performed at 23±1°C.

Table 2 Detection criteria for gel point and vitrification point

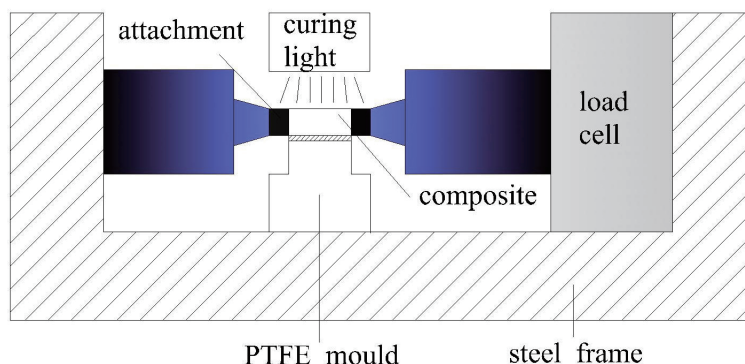| Detection criterion	Definition
Gel point 1 (G1)	Peak in shrinkage strain rate
Gel point 2 (G2)	Onset of shrinkage stress (15 mN)
Vitrification point 1 (V1)	Peak in stress rate
Vitrification point 2 (V2)	Peak in heat flow rate

Fig. 2 Schematic illustration of stress-analyzer experimental setup.

Shrinkage strain was continuously recorded for 600 s, as well as the time at which maximum shrinkage strain rate occurred. The latter could be considered as a gel point indicator (Table 2 and Fig. 3c).

Shrinkage stress measurement
1. Measurement setup
Shrinkage stress was assessed using a stress analyzer (Fig. 2)[21]. The setup comprised two identical stainless steel molds at opposing ends of composite specimen. One was connected to a 100-N load sensor (1 mN resolution, Instron, Canton, MA, USA), and the other was fixed to the steel frame of the test device.

A PTFE mold was also fixed to the test device. Composite attachments made of CharmFil composite (DentKist Inc., Seoul, Korea) were placed at both sides of PTFE mold, parallel to each other and 6 mm apart. A simulated cavity of 2×2×6 mm was thus built up between these two composite attachments. C-factor was calculated to be 0.2. Before each measurement, these attachments were replaced with a new pair and the latter polymerized for 40 s using LED curing light (Bluephase).

2. Measurement procedure
Before each measurement, a layer of adhesive (P90 System Adhesive, 3M ESPE, Seefeld, Germany) was uniformly applied on the inner walls of the cavity and light-cured for 20 s using the LED curing light (Bluephase) at 650 mW/cm². Composite resin was placed in the cavity in bulk and then light-cured from the top at 3 mm distance using the LED curing light (Bluephase) for 30 s at 650 mW/cm². Shrinkage force (N) was continuously recorded for 600 s after start of irradiation

(*n*=10 per composite material). Shrinkage stress values were calculated from recorded shrinkage force values. All measurements were performed at 23±1°C.

Stress rate of each composite material was obtained by calculating the derivative of its smoothed stress-time curve. Maximum stress rates (expressed as MPa/s) during and after LED light exposure were obtained from the stress-time curves (Fig. 4c).

As a composite material gels, forces build up within the material. Therefore, gel point can be determined based on the force value. In this experiment, the time at which force value reached 15 mN was considered as an indirect indication of gel point (Table 2). This force value must be attained at a safe distance from background noise. In this study, noise level from the machine was 10 mN, thereby rendering 15 mN to be at a safe distance from the background noise. On vitrification points, the maximum stress rate manifested during light exposure could be regarded as a logical indicator of vitrification (Table 2 and Fig. 4c).

Heat flow measurement
A modified photo-DSC apparatus[22] (CDR-4P, Shanghai Precision & Scientific Instrument Co., Ltd., Shanghai, China) was positioned directly above the specimen pan to measure heat flow when composite specimen was exposed to LED curing light (Bluephase). Conversely, the reference pan was kept empty. All measurements were performed isothermally at 23±1°C.

Each composite specimen (10±0.1 mg) was light-cured from the top at 5 mm distance using the LED curing light (Bluephase) for 30 s at 650 mW/cm². Data acquisition rate was 10 s⁻¹. Maximum heat flow rate and
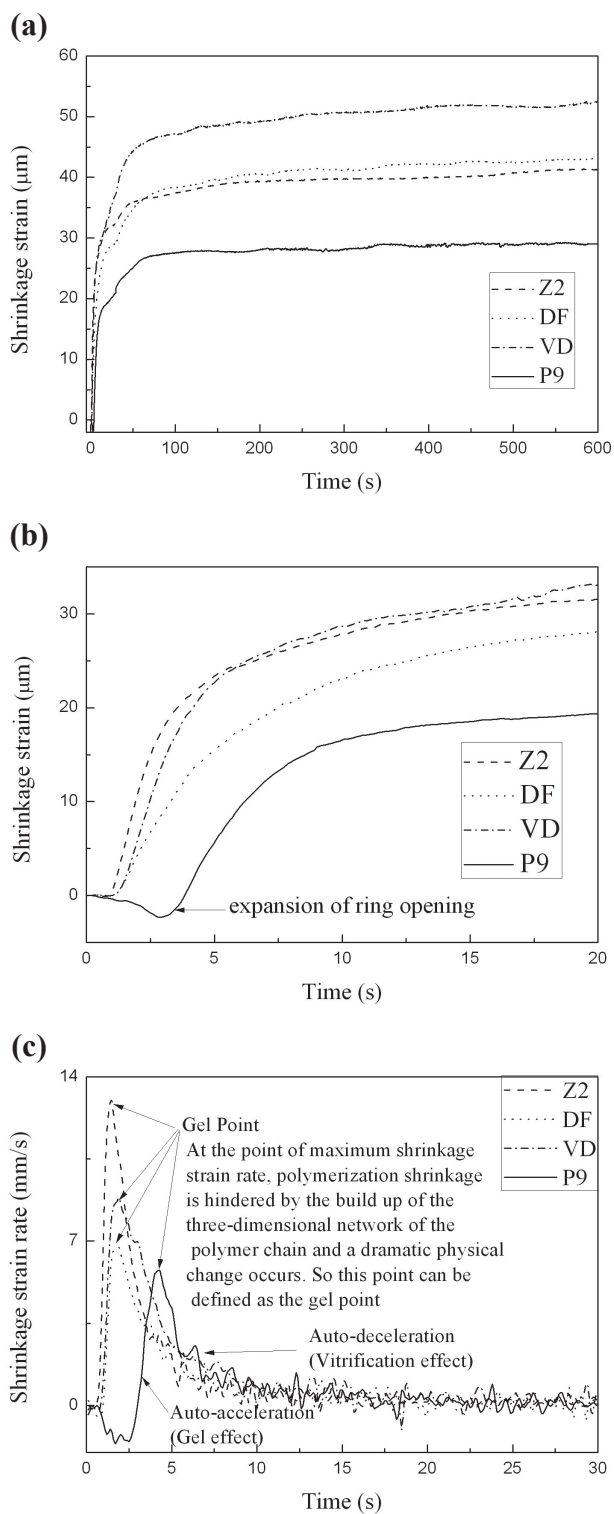
Fig. 3   (a) Shrinkage strain throughout 600 s after start of irradiation; (b) Magnified view for initial 20 s; (c) Shrinkage strain rate and gel point.
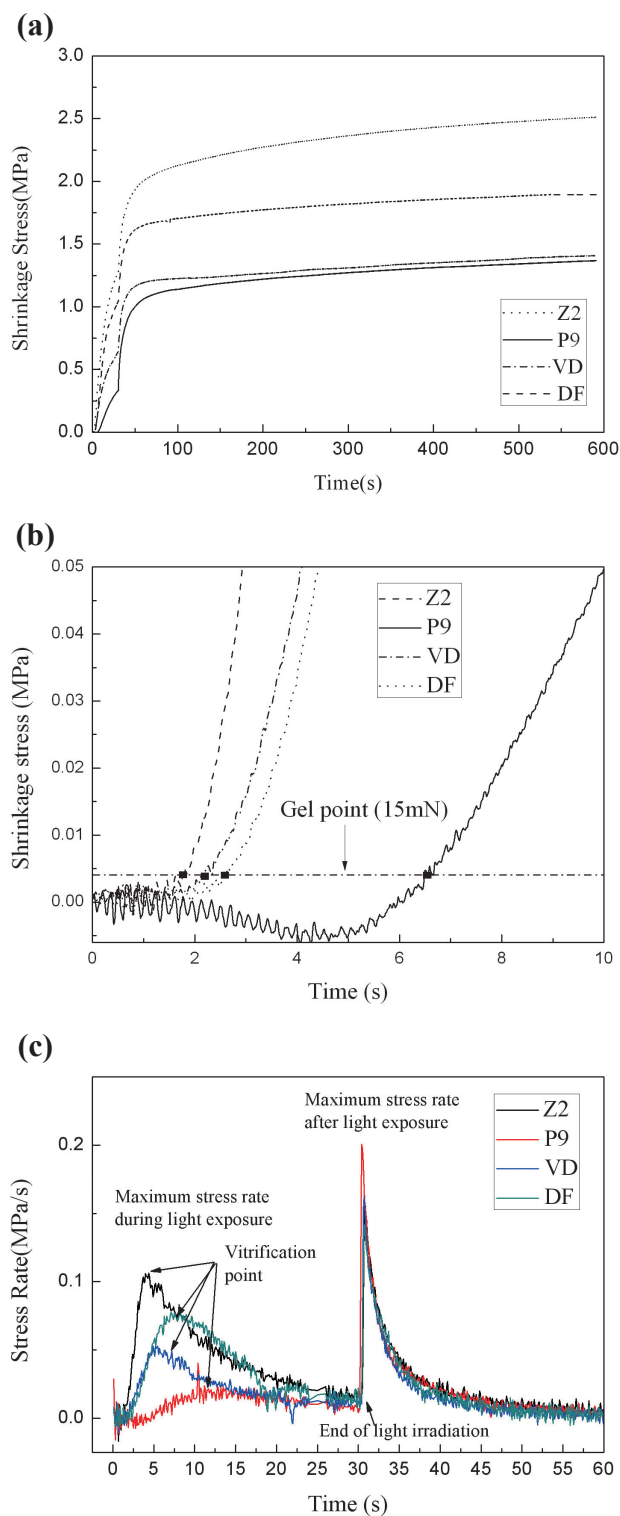
Fig. 4   (a) Shrinkage stress throughout 600 s after start of irradiation; (b) Magnified view for initial 10 s; (c) Shrinkage stress rate and gel point.

time to maximum heat flow were acquired after continuous recording for 60 s. On vitrification points, the time at which peak heat flow rate was reached could also be used as an indicator of vitrification (Table 2).

Statistical analysis
According to each composite material, data were evaluated for statistical significance (p=0.05) by one-way ANOVA and Tukey's *post hoc* test. Correlation analysis was done to investigate the relationship between Gel point 1 and Gel point 2, and between Vitrification point 1 and Vitrification point 2.

RESULTS

Shrinkage strain
Figure 3a presents the representative axial shrinkage strain curves of the four composite materials. Their shrinkage strain rate curves are presented in Fig. 3c. Shrinkage started as soon as light-curing commenced for Z2, DF, and VD. Interestingly for P9, a dilatation peak occurred during the first few seconds of light-curing (Fig. 3b).

Soon after the initial few seconds of light-curing, shrinkage rapidly increased. It reached an initial plateau until curing light was turned off, and then increased again. Slowly, a final plateau was reached.

After 600 s, shrinkage strain values of composite materials in descending order were given as follows: VD (49.4 μm)>DF (43.7 μm)>Z2 (43.1 μm)>P9 (29.1 μm). There was no significant difference between Z2 and DF (p>0.05) (Table 3).

Shrinkage stress and stress rate
Figure 4a presents the representative shrinkage stress curves of the four composite materials. Stress started to increase at approximately 1–3 s after light-curing commenced for Z2, DF, and VD (Fig. 4b). For P9, no large increase in stress was observed until at about 6 s after light exposure. After 600 s, P9 (1.38 MPa) and VD (1.41 MPa) presented the lowest values, and they were significantly different (p<0.05) from DF (1.85 MPa). Z2 (2.53 MPa) showed the highest shrinkage stress.

Figure 4c presents the shrinkage stress rate curves of the four composite materials. Maximum stress rates during and after light exposure are also listed in Table 3.

During light exposure, Z2 exhibited the highest maximum stress rate (0.138 MPa/s) whereas P9 exhibited the lowest (0.04 MPa/s). After light exposure, P9 exhibited the highest maximum stress rate (0.25 MPa/s), which was even higher than the highest maximum stress rate exhibited by Z2 during light exposure. For VD, DF and Z2, there were no significant differences (p>0.05) in post-exposure maximum stress rate among them.

Heat flow
Figure 5 presents the heat flow rate curves of the four composites during and after light exposure. These curves represented the exothermic curves due to photopolymerization. Maximum heat flow rates are also listed in Table 3. P9 showed the highest heat flow rate (8.39 mW/mg) compared to Z2 (5.07 mW/mg), DF (4.51 mW/mg), and VD (4.74 mW/mg). There was no significant difference between DF and VD (p>0.05) (Table 3).

Gel point and vitrification point
Detection criteria for both gel point and vitrification point are summarized in Table 2. Gel and vitrification times obtained for the four composites are presented in Table 4, Fig. 3c, and Fig. 4c. Correlation analysis showed
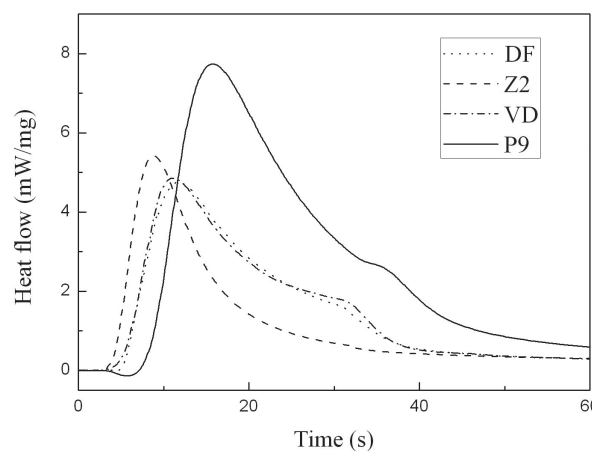

Fig. 5 Heat flow rate during and after light exposure for 60 s.

Table 3 Shrinkage strains, shrinkage stresses, stress rates, and heat flow rates of composite materials

Composite	Maximum shrinkage strain (μm)	Maximum shrinkage stress (MPa)	Maximum stress rate (MPa/s)		Maximum heat flow rate (mW/mg)
			During light exposure	After light exposure	
P9	29.1(1.8)[A]	1.38(0.05)[A]	0.040(0.003)[A]	0.250(0.023)[A]	8.39(0.53)[A]
VD	49.4(1.5)[B]	1.41(0.08)[A]	0.075(0.008)[B]	0.178(0.011)[B]	4.74(0.28)[B]
DF	43.7(2.3)[C]	1.85(0.06)[B]	0.108(0.010)[C]	0.188(0.010)[B]	4.51(0.26)[B]
Z2	43.1(1.4)[C]	2.53(0.10)[C]	0.138(0.025)[D]	0.185(0.012)[B]	5.07(0.31)[C]

Same superscript letters in each column indicate that mean values are not significantly different (p>0.05).

Table 4   Gel points and vitrification points of composite materials

Composite	Gel point 1, G1 (s)	Gel point 2, G2 (s)	Vitrification point 1, V1 (s)	Vitrification point 2, V2 (s)
P9	5.9(0.6)[A]	4.2(0.3)[A]	14.5(1.1)[A]	14.6(1.0)[A]
VD	2.4(0.2)[B]	2.3(0.3)[B]	6.1(0.3)[B]	11.4(0.7)[B]
DF	2.5(0.3)[B]	1.9(0.2)[B]	8.4(0.6)[C]	12.9(1.0)[C]
Z2	1.6(0.1)[C]	1.5(0.1)[C]	4.8(0.5)[D]	9.2(0.9)[D]

Same superscript letters in each column indicate that mean values are not significantly different ($p>0.05$).
Correlation analysis showed a strong correlation between G1 and G2 (R=0.987), V1 and V2 (R=0.924).

a strong correlation between G1 and G2, (R=0.987), and between V1 and V2 (R=0.924).

Based on data obtained in this study, gel points of the four composites were ranked in descending order as follows: P9>DF, VD>Z2. There were no significant differences between DF and VD ($p>0.05$) when measured using both detection criteria (G1 and G2).

Vitrification points of the four composites were ranked in descending order as follows: P9>DF>VD>Z2. Statistically significant differences were found between each other ($p<0.05$) in terms of both detection criteria (V1 and V2).

It could be seen that vitrification point rankings were almost the same as those for gel points, except between VD and DF for a discrepancy in vitrification point.

DISCUSSION

The hypothesis tested in this study could not be rejected because silorane-based composite (P90) did present behaviors that were markedly different from methacrylate-based composites: lowest shrinkage strain, lowest stress rate during light exposure, highest stress rate after light exposure, highest heat flow rate, and the longest gel and vitrification times. However, it must be pointed out that P9 did not wield a significant advantage ($p>0.05$) over VD on shrinkage stress as they presented similar values (Table 3).

In the present work, two detection criteria for gel point and two detection criteria for vitrification point were applied (Table 2). This is because gelation and vitrification during polymerization can be detected through changes in the dynamic developments of shrinkage stress, shrinkage strain, and heat flow. In general, G1 data corroborated G2 data and V1 data corroborated V2 data. Correlation analysis also revealed strong correlations between G1 and G2, and between V1 and V2. Interestingly though, G1 data and G2 data were strikingly similar. This could be because both the strain measuring system and stress measuring system used in our study recorded horizontal shrinkage strain or stress from the lateral surface of composite, which was perpendicular to the illumination direction. Identical experimental conditions could have also further contributed to these similar gel point data. Specimen geometry and illumination condition were the same for both shrinkage stress and strain measurements.

Further on experimental conditions, both the curing light and composite placement technique were kept the same throughout the entire experiment. Therefore, shrinkage stress development of the dental composites in our study was influenced by material compositional factors (*i.e.*, monomer, filler, and initiator system), polymerization reaction mechanism and thermal expansion, and system compliance and test configuration factors (*i.e.*, compliance of measuring instruments and C-factor)[11,23,24].

Influence of material compositional factors
Monomer composition and filler type and content can greatly influence shrinkage strain, elastic modulus, gel and vitrification times of composite resins[15,25,26]. For shrinkage stress, it is mainly dependent on the chemical composition of the composite resin.
1. P9
In the present study, P9 exhibited the lowest shrinkage strain, which was in agreement with previous findings[14]. According to Weinmann *et al.*[14], the ring-opening polymerization mechanism of oxirane moieties in the silorane monomer was responsible for the reduced shrinkage. Therefore, the polymerization shrinkage of P9 did not start immediately after light exposure, but an expansion occurred instead (Fig. 3b). Similar phenomenon was also found on the shrinkage stress curve and heat flow curve, all stemming from the cationic ring-opening polymerization of silorane-based resin[14] which was different from the free radical polymerization of methacrylate-based composites.

P9 took the longest time to reach gel and vitrification points. One hypothesis for this behavior was that siloranes were slower to polymerize, hence resulting in longer gel and vitrification times. Recent studies have shown that because of the time needed for cation formation, siloranes have a polymerization reaction with a slow onset[27,28]. By being slower to polymerize, more time is allowed for flow of material and stress relaxation. This meant that the silorane composite possessed the highest potential for stress relief by permitting material flow during the initial curing stage. As to why P9 had a similar shrinkage stress value as VD, it could be attributed to its high elastic modulus[18].
2. Z2
Z2 is a heavily filled hybrid resin composite and is rather transparent. The transparent character and choice of photoinitiator system affect the kinetics of the

polymerizing reaction in such a way that Z2 is among one of the fastest curing resin composites[29]. A faster polymerization rate means that the resin composite has a fast growth of elastic modulus and a fast development of shrinkage stress. Therefore in this study, Z2 showed the highest stress rate during light exposure and the earliest gel and vitrification points. In other words, Z2 had the highest shrinkage stress not because it had relatively high elastic modulus, unlike P9 which had a similar shrinkage stress value as VD because of its high elastic modulus.

3. VD

VD contains a novel monomer (TCD-di-HEA, (Bis-(acryloyloxymethyl)tricyclo[5.2.1.02,6]decane) in its composition. According to the manufacturer, VD has a slow cure rate because of the steric hindrance effect of the large ring structure. This explained why VD presented a relatively lower shrinkage stress (almost similar to that of P9) and long gel and vitrification times.

VD contains high molecular weight TCD monomer, but no low molecular weight diluents. Hence, its glass transition temperature is reduced and a higher degree of conversion can be achieved prior to vitrification[30]. According to Boaro *et al.*[18], VD had a low elastic modulus not only because of a lower concentration of carbon double bonds, but also because of a lower degree of conversion and a less crosslinked polymer. This explained why VD has a low elastic modulus despite an elevated filler volume fraction (64 vol%; Table 1).

Taken together, the reduced shrinkage stress of VD was ascribed to longer gel and vitrification times and a low elastic modulus.

4. DF

DF is a micro-filled resin composite, which has a lower filler volume fraction (40 vol%) than hybrid resin composite Z2 (60 vol%). Accordingly, shrinkage stress and elastic modulus were expected to be low. However, much of the filler is added to the resin matrix in prepolymerized clusters, resulting in the shrinkage strain level of DF to be similar to that of Z2. Intriguingly too, DF showed higher shrinkage stress than VD, considering its lower elastic modulus and shrinkage strain. This could be due to the higher stress rate of DF than VD.

Influence of thermal expansion on shrinkage stress
Shrinkage stress curves in Fig. 4a revealed an S-shape. During this phase, thermal expansion stress interfered with shrinkage stress. To be free from the influence of thermal expansion stress, shrinkage force was recorded for 600 s in this study to eliminate the thermal stress effect.

Thermal expansion stress is a function of the exothermic polymerization reaction of composites and heat output from the curing light[31]. It thwarts polymerization shrinkage stress, is able to slow down and even stop temporarily. However, a sudden drop in temperature after light exposure produces thermal shrinkage, which when added to polymerization shrinkage, causes a sharp upward bend of the shrinkage

stress curve. This effect also caused the highest shrinkage stress rate (Table 3). P9 had the highest shrinkage stress rate after light exposure. This was probably because P9 had the highest heat flow rate, which meant that it liberated the largest quantity of heat during curing. By the same argument, P9 would present the largest thermal contraction.

Influence of polymerization reaction mechanism
In this study, the curing light and irradiation conditions were kept the same for all composites. The substantially different heat flow pattern of P9 most probably stemmed from its different polymerization reaction mechanism — namely, the cationic ring-opening polymerization reaction of siloxane and oxirane moieties in P9. According to Miletic *et al.*[19], P9 had a different temperature curve with significantly higher temperatures when compared to ormocer- and dimethacrylate-based composites. This implied that the cationic ring-opening polymerization reaction of P9 posed a different heat generation pattern. Similarly, an optical pyrometry study[32] showed that the cationic ring-opening polymerization reaction of oxiranes was a highly exothermic one. Temperature could soar from room temperature to that above 100°C within seconds.

It has become apparent that due to its different resin formulation, P9 liberated a higher quantity of heat during curing because of a different polymerization reaction mechanism. P9 also had a faster shrinkage stress development after light exposure. The latter phenomenon thus raises the question of the effect of this considerable stress development on the interface between the cavity wall and the composite restorative.

Influence of C-factor
C-factor has been shown to be an influential factor toward shrinkage stress[23]. In this study, the C-factor was very low (0.2). For this reason, our experimental setup did not include a feedback system, whereas compliance compensation should be mandatory if C-factor were high or test molds with different configuration factors were used for evaluation[25].

In a study by Boaro *et al.*[18] which used a universal testing machine with a feedback mechanism to measure shrinkage stress, light exposure was set at approximately 570 mW/cm²×32 s —irradiation conditions which were similar to those used in this study. They reported a higher shrinkage stress than that obtained in the present study. Since the curing conditions were similar, it should be the C-factor which accounted for the different results. Their C-factor of reference was 3, which was markedly higher than that used in the present study. A low C-factor indicates more unbonded or free surface of the composite, which means more chance for material flow. More free surface is tantamount to a smaller restriction to shrinkage, which then results in reduced stress[33].

Apart from influencing the amount of stress generated, C-factor also contributed toward shrinkage stress rankings among composites. In this study, Z2 showed the highest shrinkage stress, DF came in second,

while P9 and VD exhibited the lowest shrinkage stress. Interestingly, shrinkage stress rankings after 5 min in C-factor=3[18] were as follows: P9 (4.3 MPa)>Z2 (3.3 MPa)>VD (2.8 MPa)>DF (2.6 MPa). In another study[17] (C-factor=0.5; no feedback mechanism; irradiation conditions: 500 mW/cm^2 × 40 s), P9 (0.9 MPa) showed statistically higher stress than VD (0.6 MPa), but lower than Z2 (1.1 MPa).

C-factor affects a material's ability to flow and relieve stress during the initial moments of curing. Low C-factors are favorable to stress relief: more free surface for material flow and less restriction to bulk shrinkage. Therefore, if a material is able to provide significant stress relief, shrinkage stress development would be slower and lower stress would be generated. This means that a possible reason for the different stress rankings above was due to the varied stress-relief properties among the composites. Composites with superior stress-relief properties would possess an apparent advantage over composites with inferior stress-relief properties. In this study, P9 showed the longest gel and vitrification times, which meant that P9 had the longest time to relieve stress. Coupled with a low C-factor of 0.2, P9 featured the lowest shrinkage stress, which did not agree with the findings of previous studies[17,18].

Shrinkage stress is a dynamic phenomenon. It is neither a local physical state nor a static fundamental property. The amount of shrinkage stress generated depends on specimen geometry and boundary conditions. Within the limitations of this *in vitro* study, it is reasonable to suggest that when instrumental C-factor was low, gel and vitrification points played a more important role toward shrinkage stress development and that the generated shrinkage stress was also lower. As to whether the gel point or vitrification point would exert a greater effect would depend on the experimental setup.

CONCLUSIONS

Within the limitations of this study, the following conclusions were drawn:

1. Compared to methacrylate-based composites, low-shrinkage silorane-based composite (Filtek P90) demonstrated improvements with delayed gel and vitrification points and reduced shrinkage strain.

2. Compared to a low-shrinkage composite (Venus Diamond), the silorane-based composite did not show significant shrinkage stress reduction.

3. Due to considerable heat generation during cationic ring-opening polymerization, the silorane-based composite showed a significantly higher stress rate after light exposure.

REFERENCES

1) Feilzer AJ, De Gee AJ, Davidson CL. Quantitative determination of stress reduction by flow in composite restorations. Dent Mater 1990; 6: 167-171.
2) Davidson CL. Resisting the curing contraction with adhesive composites. J Prosth Dent 1986; 55: 446-447.
3) Davidson CL, Feilzer AJ. Polymerization shrinkage and polymerization shrinkage stress in polymer-based restoratives. J Dent 1997; 25: 435-440.
4) Dauvillier BS, Aarnts MP, Feilzer AJ. Developments in shrinkage control of adhesive restoratives. J Esthet Dent 2000; 12: 291-299.
5) Ferracane JL, Mitchem JC. Relationship between composite contraction stress and leakage in Class V cavities. Am J Dent 2003; 16: 239-243.
6) Visvanathan A, Ilie N, Hickel R, Kunzelmann KH. The influence of curing times and light curing methods on the polymerization shrinkage stress of a shrinkage-optimized composite with hybrid-type prepolymer fillers. Dent Mater 2007; 23: 777-784.
7) Fano L, Ma WY, Marcoli PA, Pizzi S, Fano V. Polymerization of dental composite resins using plasma light. Biomaterials 2002; 23: 1011-1015.
8) Dewaele M, Asmussen E, Peutzfeldt A, Munksgaard EC, Benetti AR, Finné G, Leloup G, Devaux J. Influence of curing protocol on selected properties of light-curing polymers: Degree of conversion, volume contraction, elastic modulus, and glass transition temperature. Dent Mater 2009; 25: 1576-1584.
9) Lange J, Altmann N, Kelly CT, Halley PJ. Understanding vitrification during cure of epoxy resins using dynamic scanning calorimetry and rheological techniques. Polymer 2000; 41: 5949-5955.
10) Lee IB, Um CM. Thermal analysis on the cure speed of dual cured resin cements under porcelain inlays. J Oral Rehabil 2001; 28: 186-197.
11) Braga RR, Ballester RY, Ferracane JL. Factors involved in the development of polymerization shrinkage stress in resin-composites: a systematic review. Dent Mater 2005; 21: 962-970.
12) Feilzer AJ, de Gee AJ, Davidson CL. Setting stress in composite resin in relation to configuration of the restoration. J Dent Res 1987; 66: 1636-1639.
13) Silikas N, Eliades G, Watts DC. Light intensity effects on resin-composite degree of conversion and contraction strain. Dent Mater 2000; 16: 292-296.
14) Weinmann W, Thalacker C, Guggenberg R. Silorane in dental composites. Dent Mater 2005; 21: 68-74.
15) Ilie N, Jelen E, Hickel R, Clementino-Luedemann T. Low-shrinkage composite for dental application. Dent Mater J 2007; 26: 149-155.
16) Papadogiannis D, Kakaboura A, Palaghias G, Eliades G. Setting characteristics and cavity adaptation of low-shrinking resin composites. Dent Mater 2009; 25: 1509-1516.
17) Marchesi G, Breschi L, Antoniolli F, Di Lenarda R, Ferracane J, Cadenaro M. Contraction stress of low-shrinkage composite materials assessed with different testing systems. Dent Mater 2010; 26: 947-953.
18) Boaro LC, Gonçalves F, Guimarães TC, Ferracane JL, Versluis A, Braga RR. Polymerization stress, shrinkage and elastic modulus of current low-shrinkage restorative composites. Dent Mater 2010; 12: 1144-1150.
19) Miletic V, Ivanovic V, Dzeletovic B, Lezaja M. Temperature changes in silorane-, ormocer-, and dimethacrylate-based composites and pulp chamber roof during light-curing. J Esthet Restor Dent 2009; 21: 122-131.
20) Gao BT, Zheng G, Lin H, Xu YX. A new dynamic approach for monitoring dental composite curing kinetics. Beijing Da Xue Xue Bao 2011; 43: 895-899.
21) Gao BT, Lin H, Han JM, Zheng G. Polymerization characteristics, flexural modulus and microleakage evaluation of silorane-based and methacrylate-based composites. Am J Dent 2011; 24: 97-102.
22) Xiao P, Shi SQ, Nie J. Synthesis and characterization of copolymerizable one-component type II photoinitiator. Polym

Adv Technol 2008; 19: 1305-1310.

23) Cunha LG, Alonso RC, Pfeifer CS, Correr-Sobrinho L, Ferracane JL, Sinhoreti MA. Contraction stress and physical properties development of a resin-based composite irradiated using modulated curing methods at two C-factor levels. Dent Mater 2008; 24: 392-398.

24) Min SH, Ferracane J, Lee IB. Effect of shrinkage strain, modulus, and instrument compliance on polymerization shrinkage stress of light-cured composites during the initial curing stage. Dent Mater 2010; 26: 1024-1033.

25) Chen HY, Manhart J, Hickel R, Kunzelmann KH. Polymerization contraction stress in light-cured packable composite resins. Dent Mater 2001; 17: 253-259.

26) Alvarez-Gayosso C, Barcelo-Santana F, Guerrero-Ibarra J, Sáez-Espínola G, Canseco-Martínez MA. Calculation of contraction rates due to shrinkage in light-cured composites. Dent Mater 2004; 20: 228-235.

27) Stansbury JW, Trujillo-Lemon M, Lu H, Ding X, Lin Y, Ge J. Conversion-dependent shrinkage stress and strain in dental resins and composites. Dent Mater 2005; 21: 56-67.

28) Ferracane JL. Developing a more complete understanding of stresses produced in dental composites during polymerization. Dent Mater 2005; 21: 36-42.

29) Hofmann N, Denner W, Hugo B, Klaiber B. The influence of plasma arc vs. halogen standard or soft-start irradiation on polymerization shrinkage kinetics of polymer matrix composites. J Dent 2003; 31: 383-393.

30) Sideridou I, Tserki V, Papanastasiou G. Effect of chemical structure on degree of conversion in light-cured dimethacrylate-based dental resins. Biomaterials 2002; 23: 1819-1829.

31) Tarle Z, Meniga A, Knezevic A, Sutalo J, Ristić M, Pichler G. Composite conversion and temperature rise using a conventional, plasma arc, and an experimental blue LED curing unit. J Oral Rehabil 2002; 29: 662-667.

32) Crivello JV, Falk B, Zonca MR. Photoinduced cationic ring-opening frontal polymerizations of oxetanes and oxiranes. J Polym Sci 2004; 42: 1630-1646.

33) Laughlin GA, Williams JL, Eick JD. The influence of system compliance and sample geometry on composite polymerization shrinkage stress. J Biomed Mater Res 2002; 63: 671-678.